

## Nitrosyl Complexes | Very Important Paper |

VIP

## The Structural Chemistry of Stable High-Spin Nitrosyl–Iron(II) Compounds with Aminocarboxylato Co-Ligands in Aqueous Solution

Bianca M. Aas<sup>[a]</sup> and Peter Klüfers<sup>\*[a]</sup>

Dedicated to Professor Wolfgang Beck on the occasion of his 85th birthday

**Abstract:** Four crystalline nitrosyl–iron compounds of the  $\{\text{FeNO}\}^7(S = 3/2)$  type with aminocarboxylato co-ligands were prepared from aqueous solutions of iron(II) sulfate, an equimolar amount of one of the co-ligands ethylenediamine-*N,N'*-diacetate (edda), nitrilotriacetate (nta), *N,N'*-bis(2-hydroxyethyl)ethylenediamine-*N,N'*-diacetate (bhedda) or ethylenediamine-*N,N,N',N'*-tetraacetate (edta) and gaseous nitric oxide. The hemihydrate  $[\text{Fe}(\text{edda})(\text{H}_2\text{O})(\text{NO})] \cdot 0.5\text{H}_2\text{O}$  (**1**·0.5H<sub>2</sub>O), a hydrated coordination polymer  $[\{\text{Fe}(\text{H}_2\text{O})_4\}\{\text{Fe}(\text{NO})(\text{nta})\}_2]_{n/n} \cdot 2\text{H}_2\text{O} = [\text{Fe}(\text{H}_2\text{O})_4(\mathbf{2})_2]_{n/n} \cdot 2\text{H}_2\text{O}$  with  $[\text{Fe}(\text{NO})(\text{nta})]^-$  (**2**) monoanions, the solvent-free complex  $[\text{Fe}(\text{bhedda})(\text{NO})]$  (**3**) and an-

other coordination polymer  $[\text{Fe}(\text{H}_2\text{O})_2\{\text{Fe}(\text{NO})(\text{Hedta})\}_2]_{n/n} = [\text{Fe}(\text{H}_2\text{O})_2(\mathbf{4})_2]_{n/n}$  with  $[\text{Fe}(\text{Hedta})(\text{NO})]^-$  (**4**) monoanions were investigated by crystallography and IR and UV/Vis spectroscopy. Structural peculiarities, such as a tilt of the NO ligand toward the O atom of a neighbouring carboxylato ligand, were analysed by DFT calculations. The stability of the aqueous solutions of the target compounds against inert-gas stripping was related to the low amount of the less stable aqua complex  $[\text{Fe}(\text{H}_2\text{O})_5(\text{NO})]^{2+}$  in the aqueous equilibria in addition to the intrinsic stability of the species.

## Introduction

The reaction of nitric oxide with iron(II) in a weak-field environment has been a focus of research for more than a century. The early investigations on the resulting mononitrosyl–iron compounds, which, according to the Enemark–Feltham notation, are quartet- $\{\text{FeNO}\}^7$  species, were motivated by the attempt to elucidate the chromophore of the brown-ring test for nitrate detection and the same chromophore in nitrite analysis. The pioneering work of Kohlschütter and Manchot before World War I was thus devoted to simple aqua and halogenido species; their work has been included in more detail in the accompanying article on less stable centres of this kind.<sup>[1]</sup>

Decades later, aminocarboxylato co-ligands were discovered to induce a markedly increased stability of the quartet- $\{\text{FeNO}\}^7$  centres against NO release. Hence, particularly the edta spectator ligand was frequently employed for the preparation of stable solutions which were investigated for various reasons. In the 1980s, NO absorption in Fe<sup>II</sup>/edta solutions were developed as a method for stripping NO from power plant flue-gas streams. As the scientific goal, the identification of the species

as mononitrosyl (instead of dinitrosyl) entities was questioned.<sup>[2]</sup> In the 1990s, the focus shifted to attempts to understand the bonding mode within the Fe(NO) chromophore. The tools used, particularly by the Solomon group, included various spectroscopic methods supported by computational procedures.<sup>[3]</sup> In this period, a view at the quartet- $\{\text{FeNO}\}^7$  moiety as a high-spin iron(III) centre antiferromagnetically coupled to a <sup>3</sup>NO<sup>-</sup> ligand emerged. In the early 2000s, the van Eldik group published several studies on spectroscopic and thermodynamic, as well as kinetic, data of aqueous  $\{\text{FeNO}\}^7(S = 3/2)$  complexes. Their studies provided a comprehensive view of about one hundred aminocarboxylato co-ligands, including representatives of various denticity such as edta, nta and ida.<sup>[4]</sup> Reactivity data were also given with the result that the stability of the Fe–NO linkage roughly correlates with the sensitivity of the respective aqueous solution to oxidation by O<sub>2</sub>. To master this problem on a technologically applicable level, in the most recently published investigations, a reduction step has been added to currently developed flue-gas cleaning processes. In terms of co-ligands, these currently engineered processes, for example, the chemical absorption – biological reduction (CABR) method, rely on edta.<sup>[5]</sup>

On the whole, edta appears to be the most important co-ligand, both in the application-oriented flue-gas area in engineering science, where this system is typically addressed as “Fe<sup>-</sup>EDTA-NO”, as well as in the field of basic research. In the latter context, it should be noted that the molecular structure of the tentative  $[\text{Fe}(\text{edta})(\text{NO})]^{2-}$  species was merely assumed when

[a] Department Chemie, Ludwig-Maximilians-Universität München, Butenandtstraße 5-13, 82377 München, Germany  
E-mail: kluef@cup.uni-muenchen.de  
<http://www.cup.lmu.de/ac/kluefers/homepage/>

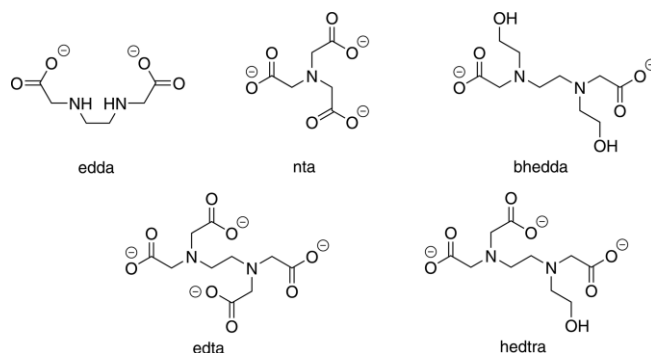
Supporting information for this article is available on the WWW under <http://dx.doi.org/10.1002/ejic.201601330>.

starting computational approaches, mostly on the basis of the heptacoordinate  $[\text{Fe}(\text{edta})(\text{H}_2\text{O})]^{2-}$  parent species prior to NO bonding. In a thorough EXAFS analysis of frozen  $\text{Fe}^{\text{II}}/\text{edta}/\text{NO}$  solutions, the authors deviated from this use by starting curve fitting on the basis of the structural parameters of the (also heptacoordinate) ferric  $[\text{Fe}(\text{edta})(\text{H}_2\text{O})]^-$  species, thus following the assumption that the  $\{\text{FeNO}\}^7$  moiety exhibits some iron(III) character. (In this study, a Fe–N–O angle of  $156^\circ$  was obtained – pretty close to the value of  $149^\circ$  presented below.)<sup>[3b]</sup> Since the  $\text{Fe}^{\text{II}}/\text{edta}/\text{NO}$  system shares the lack of structural information with all other aminocarboxylate analogues, we launched a program to crystallise the target complexes in order to provide the molecular structures as a prerequisite for future work on more solid ground.

In order to arrange our work reasonably, we used a stability argument that we derived from a result reported by the van Eldik group on the different behaviour of the various aqueous systems towards bubbling with inert gas.<sup>[4c]</sup> Starting from these quantitative analyses, we simply addressed two stability groups. On the one hand, nitrosyl species, the aqueous solutions of which lose nitric oxide on bubbling with argon within a minute, are grouped together in a low-stability class. On the other hand, those species that resist this procedure are combined in a stable group of quartet- $\{\text{FeNO}\}^7$  species. At the same time, all members of the stable group also resist vacuum for the same period of time. This publication is devoted to this stable group, which contains aminocarboxylates of denticity four and higher. Moreover, the typical bonding situation is analysed in some depth in the accompanying publication on the less stable iron–nitrosyl compounds.<sup>[1]</sup> Remarkably, the bonding analysis presented there turns out to be essentially the same here for the aminocarboxylate co-ligands. Specifically, the quartet- $\{\text{FeNO}\}^7$  species are suitably described as intermediate, between a high-spin- $\text{Fe}^{\text{II}}(\text{NO})$  and a high-spin- $\text{Fe}^{\text{III}}(\text{NO}^-)$  state, both of which exhibit a strong antiferromagnetic coupling of the excess spins of the transition metal and the ligand. Moreover, an argument for the oxidation state of the central atom, based on atomic distances, supplements the DFT and CASSCF results. We start the “Results and Discussion” section with the description of the molecular structures of four aminocarboxylate/ $\text{Fe}/\text{NO}$  compounds of the stable class that retained the dark-green colour of the mother liquors when treated with an inert-gas stream or when subjected to low pressure.

## Results and Discussion

Dark-green quartet- $\{\text{FeNO}\}^7$  compounds with ethylenediamine- $N,N'$ -diacetate (edda), nitrilotriacetate (nta),  $N,N'$ -bis(2-hydroxyethyl)ethylenediamine- $N,N'$ -diacetate (bhedda) and ethylenediamine- $N,N,N',N'$ -tetraacetate (edta) co-ligands (Scheme 1) were synthesised from ferrous sulfate heptahydrate and sodium or potassium hydroxide with the free acid of the aminocarboxylate co-ligand and nitric oxide gas in aqueous solution. Crystallisation succeeded by the diffusion of acetone or ethanol into the aqueous solutions.



Scheme 1. Aminocarboxylate co-ligands mentioned in this work: ethylenediamine- $N,N'$ -diacetate (edda), nitrilotriacetate (nta),  $N,N'$ -bis(2-hydroxyethyl)ethylenediamine- $N,N'$ -diacetate (bhedda), ethylenediamine- $N,N,N',N'$ -tetraacetate (edta) and ( $N$ -hydroxyethyl)ethylenediaminetriacetate (hedtra).

## Crystal and Molecular Structures

### $[\text{Fe}(\text{edda})(\text{H}_2\text{O})(\text{NO})] (1)$

The tetradentate edda ligand gave rise to an octahedral nitrosyl complex, the single free coordination site of which is occupied by an aqua ligand. The molecular structure of the greenish-black crystals of  $1 \cdot 0.5\text{H}_2\text{O}$  is shown in Figure 1. The asymmetric unit contains two symmetrically independent molecules that do not significantly differ from each other in terms of angles and distances; hence, only one molecule is depicted.

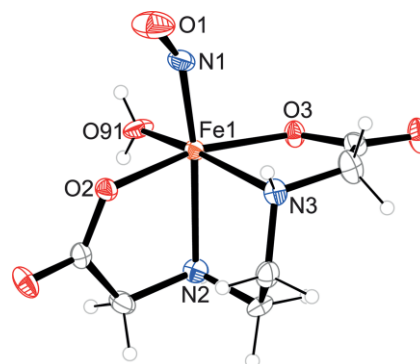
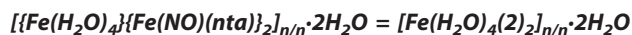


Figure 1. ORTEP plot of one of two symmetrically independent molecules of **1** (50 % probability level). Interatomic distances (in Å) and angles (in  $^\circ$ ) with the standard deviation of the last digit in parentheses: Fe1–N1 1.775(3), Fe1–O2 2.004(2), Fe1–N3 2.173(3), Fe1–N2 2.231(3), Fe1–O3 2.086(2), Fe1–O91 2.070(3), N1–O1 1.163(3), Fe1–N1–O1 147.8(3), N1–Fe1–O2 89.93(11), N1–Fe1–O91 97.26(13), N1–Fe1–O3 101.07(11), N1–Fe1–N3 97.03(12), N1–Fe1–N2 168.61(12). Data of the second independent complex molecule: Fe1'–N1' 1.775(3), Fe1'–O2' 2.019(2), Fe1'–N3' 2.165(3), Fe1'–N2' 2.229(3), Fe1'–O3' 2.089(2), Fe1'–O91' 2.058(3), N1'–O1' 1.158(3), Fe1'–N1'–O1' 148.5(2), N1'–Fe1'–O2' 90.23(11), N1'–Fe1'–O91' 95.53(13), N1'–Fe1'–O3' 100.78(11), N1'–Fe1'–N3' 97.28(12), N1'–Fe1'–N2' 168.43(11).

The  $C_2$ -symmetric, tetradentate ligand leaves a *cis* coordination site at the iron centre. As a result, nitric oxide and the aqua ligand coordinate *trans* to an edda nitrogen atom. General features that are shared by the other compounds include the deviation of the nitrosyl–iron moiety from linearity, the inclination of the  $\text{FeNO}$  group as a whole toward the carboxylate functions, and the tilt of the NO ligand in the same direction. These topics will be addressed later.



Greenish-black crystals of the coordination polymer  $[\{\text{Fe}(\text{H}_2\text{O})_4\}\{\text{Fe}(\text{NO})(\text{nta})\}_2]_{n/n} \cdot 2\text{H}_2\text{O}$  with  $[\text{Fe}(\text{NO})(\text{nta})]^-$  (**2**) as the nitrosyl-containing building block were obtained from equimolar solutions of ferrous sulfate and partly neutralised nitrilotriacetic acid in a rather time-consuming procedure (see Experimental Section). Crystal-structure analysis revealed a higher Fe/nta molar ratio than the supplied 1:1 proportion. However, the equimolar ratio is preserved in the nitrosyl-containing  $[\text{Fe}(\text{nta})(\text{NO})]^-$  anion. The entire crystal is a "higher-order" coordination polymer. First, pentacoordinate  $[\text{Fe}(\text{nta})(\text{NO})]^-$  building units attain hexacoordination by forming a one-dimensional, zig-zag-shaped polyanion, which provides lateral carboxylate-O atoms. Second, the lateral donor functions complete planar dicationic  $\text{Fe}(\text{H}_2\text{O})_4$  moieties – instead of the attempted sodium counterions – to octahedra by two *trans* linkages from two parallel-arranged polyanions.

The structure of the anionic  $[\text{Fe}(\text{nta})(\text{NO})]^-$  building unit is illustrated in Figure 2. As with **1**, the tetradentate chelate ligand leaves a *cis* coordination site at the central metal. The nitrosyl group is bound *trans* to the nitrogen atom of the co-ligand. The carboxylate function from the adjacent anion that fills the sixth coordination site is drawn as well.

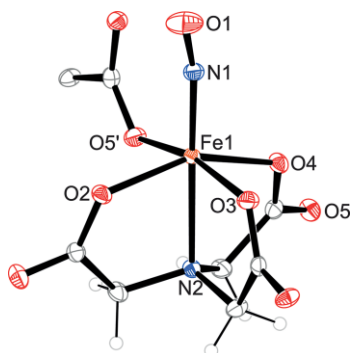


Figure 2. ORTEP plot of the anion **2** including a carboxylate residue of the adjacent anion (50 % probability level). Interatomic distances (in Å) and angles (in °) with the standard deviation of the last digit in parentheses: Fe1–N1 1.752(3), Fe1–O2 2.072(2), Fe1–N2 2.226(3), Fe1–O3 2.055(2), Fe1–O4 2.086(2), Fe1–O5 2.073(2), N1–O1 1.152(3), Fe1–N1–O1 164.8(3), N1–Fe1–O2 99.01(11), N1–Fe1–O5 100.80(11), N1–Fe1–O4 106.79(11), N1–Fe1–O3 93.21(11), N1–Fe1–N2 172.93(11).

### $[\text{Fe}(\text{bhedda})(\text{NO})]$ (**3**)

The crystallisation of a Fe/bhedda/NO complex from aqueous solution was hampered, but it succeeded with methanol as the reaction medium. Structure analysis on a solvent-free, brownish-black crystal revealed mononuclear coordination entities. In Figure 3, the potentially hexacoordinate bhedda ligand is shown to act in a pentacoordinate bonding mode by using its carboxylate and amino functions, but leaving one of the two hydroxyethyl functions dangling. As a result, octahedral coordination on nitric oxide binding is achieved.

In compound **3**, a peculiarity of the structures in this work becomes distinct, namely the normal shape of the thermal ellipsoid of the nitrosyl O atom. However, a markedly anisotropic shape as well as disorder was usually found among the less

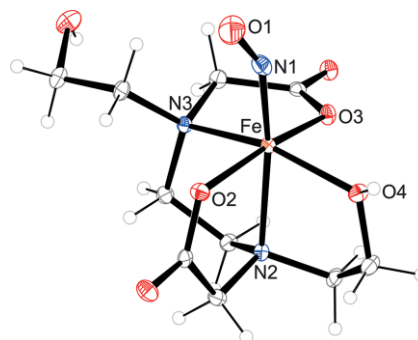


Figure 3. The molecular structures of the solvent-free mononuclear entities in crystals of **3** (50 % thermal ellipsoids). Interatomic distances (in Å) and angles (in °) with the standard deviation of the last digit in parentheses: Fe1–N1 1.782(2), Fe1–O2 2.026(1), Fe1–N3 2.242(2), Fe1–N2 2.215(2), Fe1–O3 2.045(1), Fe1–O4 2.079(1), N1–O1 1.134(2), Fe1–N1–O1 150.20(15), N1–Fe1–O2 89.90(6), N1–Fe1–O4 103.95(6), N1–Fe1–O3 101.82(6), N1–Fe1–N3 98.99(6), N1–Fe1–N2 169.22(6).

stable analogues – in line with the DFT result that the Fe–N–O bending potential is flat.<sup>[1]</sup> It was thus expected that the typical bending curve would show a more pronounced minimum close to the experimentally determined value. We thus scanned the Fe–N–O angle in  $[\text{Fe}(\text{bhedda})(\text{NO})]$  by a DFT approach (tpssh/def2-TZVP). The dependence of the energy on the tilt angle is shown in Figure 4. In fact, the experimentally determined value resembles the energy minimum. However, as in the case of the less stable complexes, the same flat bending potential results, showing an energy change of only 2.5 kJ mol<sup>−1</sup> for an angle range of 140° to 180°. A subsequent check as to whether or not the NO ligand in **3** is untypically fixed by short intermolecular contacts did not show, as usual, any of these interactions.

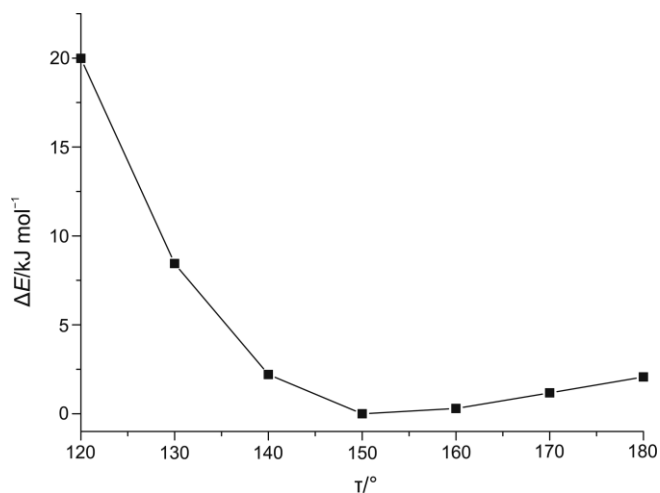
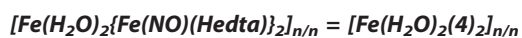


Figure 4. A relaxed  $\Delta E$  vs.  $\tau$  scan at the TPSSH/def2-TZVP level of theory;  $\tau$  is the Fe–N–O angle for  $[\text{Fe}(\text{bhedda})(\text{NO})]$  (**3**).



The potentially hexacoordinate edta ligand forms  $\{\text{FeNO}\}^7$  solutions of pronounced stability towards NO loss upon stripping with argon (note the concomitant sensitivity towards oxygen and the possibility to suppress oxidation by fluoride<sup>[6]</sup>). The crystallisation of an Fe/edta/NO complex succeeded in the

course of a similar procedure to that with **2**. Starting with an equimolar solution of ferrous salt and approximately half-neutralised ethylenediaminetetraacetic acid, we obtained a coordination polymer with higher Fe/edta molar ratio than that supplied over a prolonged period of time.

Figure 5 shows the structure of the nitrosyl-containing monoanions **4** in crystals of  $[\text{Fe}(\text{H}_2\text{O})_2\{\text{Fe}(\text{NO})(\text{Hedta})\}_2]_{n/n} = [\text{Fe}(\text{H}_2\text{O})_2(\mathbf{4})_2]_{n/n}$ . The structure of the anion closely resembles that of **3**. Instead of one hydroxyethyl function in **3**, a carboxymethyl function is dangling and results in a pentadentate Hedta ligand, leaving a coordination site for nitric oxide, which is bonded *trans* to an edta nitrogen atom.

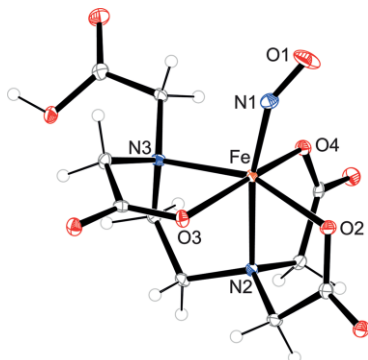


Figure 5. ORTEP plot of the  $[\text{Fe}(\text{edtaH})(\text{NO})]^-$  (**4**) monoanions in crystals of  $[\text{Fe}(\text{H}_2\text{O})_2(\mathbf{4})_2]_{n/n}$  (50 % thermal ellipsoids). Interatomic distances (in Å) and angles (in °) with the standard deviation of the last digit in parentheses: Fe1–N1 1.763(2), Fe1–O2 2.055(2), Fe1–N3 2.241(2), Fe1–N2 2.196(2), Fe1–O3 2.069(2), Fe1–O4 1.999(2), N1–O1 1.158(2), Fe2–O5 2.141(1), Fe2–O7 2.108(1), Fe2–O91 2.128(2), Fe1–N1–O1 148.8(2), N1–Fe1–O2 94.95(7), N1–Fe1–O4 91.70(7), N1–Fe1–O3 102.11(7), N1–Fe1–N3 106.37(7), N1–Fe1–N2 168.53(7).

It should be noted that, in the crystalline state, the NO-free precursor complex  $[\text{Fe}^{\text{II}}(\text{edta})(\text{H}_2\text{O})]^{2-}$  is heptacoordinate as is the  $\text{Fe}^{\text{III}}$  analogue.<sup>[7]</sup>

As with nta, the edta complex crystallises as a coordination polymer. However, the bonding motifs differ. Anion–anion bonds are lacking. (Note that octahedral **4** lacks the reason for these bonds in **2**, namely pentacoordination within the nitrosyl–iron moiety.) Instead, two-dimensional building blocks made up by diaquairon(II) cations instead of the attempted potassium counterions and anions **4** form layers along [001]. Within the 2D blocks, a square net of  $[\text{Fe}(\text{H}_2\text{O})_2]^{2+}$  building units is connected via iron–carboxylate contacts to a square anion assembly above and a square anion assembly below, resulting in the  $\text{AB}_2$ -type stoichiometry of the compound.

The mother liquor of the  $[\text{Fe}(\text{H}_2\text{O})_2(\mathbf{4})_2]_{n/n}$  species should exhibit fairly acidic conditions to support the dangling non-deprotonated carboxymethyl function. Table 1 summarises the pH-values of aqueous reaction solutions containing the species **1–4** before and after the treatment with nitric oxide. As the pH range before NO absorption lay between 3 and 6, pH values of

Table 1. Aqueous reaction solution pH values for batches containing **1–4** before and after NO absorption.

	<b>1</b>	<b>2</b>	<b>3</b>	<b>4</b>
Before NO treatment	6	3–4	4	3–4
After NO treatment	5–6	5	5–6	4–5

about 4–6 were measured after the reaction with NO. As a matter of fact, all solutions showed slightly acidic conditions. (It should be noted that the use of buffers is avoided in our experiments due to the pronounced tendency of buffer components to crystallise.)

## IR and UV/Vis Spectroscopy

The formation of the  $\{\text{FeNO}\}^7(S = 3/2)$  compounds in solution was traced by IR and UV/Vis spectroscopy. The obtained solution data agree with those reported by the van Eldik group<sup>[4c]</sup> as well as with data collected on the crystalline compounds of this work. The UV/Vis spectra show two charge-transfer bands around 300 and 400 nm and a d–d transition band around 600 nm. The characteristic N–O stretching vibration lies in the range between 1760 and 1800  $\text{cm}^{-1}$ . As in the case of the less stable aminocarboxylate complexes, the IR and UV/Vis data match published results for octahedral  $\{\text{FeNO}\}^7(S = 3/2)$  complexes.<sup>[8]</sup> Table 2 gives an overview of the measured IR and UV/Vis data for solutions as well as for the crystalline compounds of this work.

Table 2. IR- and UV/Vis-spectroscopic data; sol: the mother liquors as described in the Experimental Section; cry: solid-state measurements on crystals containing the nitrosyl moieties **1–4**. The absorption maxima given in the cry column were determined from Kubelka–Munk<sup>[9]</sup> transformed reflectance spectra. (Data for solid-state measurements on **3** are missing due to the low crystal yield.)

	$\nu(\text{NO}) / \text{cm}^{-1}$ (sol)	$\nu(\text{NO}) / \text{cm}^{-1}$ (cry)	$\lambda / \text{nm}$ (sol)	$\lambda / \text{nm}$ (cry)
<b>1</b>	1769	1761	342, 435, 617	414, 430, 644
<b>2</b>	1793	1791	339, 439, 602	433, 622
<b>3</b>	1782	–	337, 422, 650	–
<b>4</b>	1777	1781	342, 435, 634	432, 623

## DFT Calculations on **1** and **3**

DFT calculations were performed on the non-polymeric species  $[\text{Fe}(\text{edda})(\text{H}_2\text{O})(\text{NO})]$  (**1**) and  $[\text{Fe}(\text{bhedda})(\text{NO})]$  (**3**) at the tpssh/def2-TZVP level of theory. Table 3 gives an overview of the calculated and experimentally determined Fe–N and N–O distances as well as N–O stretching vibrations. The data are in good agreement. Minor deviations were found for N–O distances due to the limited reliability of the experimental positional parameters of the nitrosyl atoms in the diffraction study, that is, the inadequate approximation of the tightly bonded N and O atoms by thermal ellipsoids. The Fe–N as well as N–O distances

Table 3. Calculated and experimentally determined Fe–N and N–O distances as well as N–O stretching vibrations in the non-polymeric species  $[\text{Fe}(\text{edda})(\text{H}_2\text{O})(\text{NO})]$  (**1**) and  $[\text{Fe}(\text{bhedda})(\text{NO})]$  (**3**). Distances are in Å and frequencies are in  $\text{cm}^{-1}$ . For **1**, the experimentally determined N–O stretching vibrations from the mother liquor and from the crystalline compound are listed; for **3**, the stretching vibration of the mother liquor is given.

	Fe–N	Fe–N	N–O	N–O	$\nu(\text{NO})$	$\nu(\text{NO})$
	(calcd.)	(exp.)	(calcd.)	(exp.)	(calcd.)	(exp.)
<b>1</b>	1.78	1.78	1.17	1.16	1786	1769/1761
<b>3</b>	1.78	1.78	1.17	1.13	1791	1782

indicate the same bonding situation as for the less stable  $\{\text{FeNO}\}^7(S = 3/2)$  compounds with aminocarboxylato co-ligands, namely largely covalent Fe–NO binding through the  $\pi^*$  orbitals of the ligand and the  $d_{xz}$  and  $d_{yz}$  orbitals of the metal in an overall high-spin setup.<sup>[1]</sup>

There were some peculiarities in the compounds of this work, however, that exceeded the general bonding description in ref.<sup>[1]</sup> First, it was shown for **3** that, despite the same soft bending potential of the Fe–N–O group as for the less stable complexes, a marked anisotropy of the nitrosyl O atom in the X-ray crystallographic analyses in this work was either absent or weak. Moreover, with the exception of **2**, the Fe–N–O angles mark the lower limit of values typical for quartet- $\{\text{FeNO}\}^7$  centres.<sup>[1,8]</sup>

Second, with the structure determinations of this work, a special feature of  $\{\text{FeNO}\}^7(S = 3/2)$  complexes with aminocarboxylate ligands became apparent. The nitrosyl group was bent towards the oxygen atom of a carboxylato ligand, which is perpendicular to the basal plane of the coordination octahedron (the plane normal to the NO ligand). If two such O atoms are present as a *cis* pair, the NO ligand may be tilted into the space between them (**2** and **4**).

This observation was rationalised by DFT calculations. In a first approach, the interplay of  $\sigma$ -only- and  $\pi$ -donors as co-ligands was modelled by means of the tentative ferrate  $[\text{FeF}_3(\text{NH}_3)_2(\text{NO})]^-$ . Structure optimisation resulted in a nitrosyl group that was bent towards a fluorido ligand. Among the canonical MOs, the  $\beta$ -HOMO best serves to rationalise the observed effect (Figure 6). Since the Fe–N–O angle is distinctly small in the model compound, the bonding overlap between the terminal atoms of an F–Fe–N–O moiety is obvious. Figure 6 shows the same interaction, though to a lesser extent, for **1**.

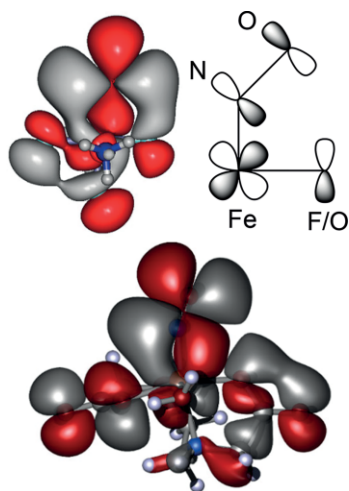


Figure 6. Top: the  $\beta$ -HOMO of the tentative  $[\text{FeF}_3(\text{NH}_3)_2(\text{NO})]^-$  model complex showing the bonding overlap of the terminal atoms of the nitrosyl and the fluorido ligand (top); bottom: the same MO for **1** (TPSSh/def2-TZVP, isovalue 0.008).

In order to quantify the effect, a relaxed scan of the rotation of the NO ligand about the Fe–N axis was performed for **1** and **3**. The result is reported in terms of four positions, namely the N–O tilt towards each of the four atoms of the equatorial plane of the complex. With the atomic labels given in Figure 1, the

experimental minimum (NO tilted towards O2, Fe–N–O<sub>exp</sub>  $\approx$  148°) is confirmed by the calculation ( $\Delta E = 0 \text{ kJ mol}^{-1}$ , Fe–N–O<sub>calcd</sub> = 152°). The conformation in which the nitrosyl ligand is tilted towards the in-plane carboxylato ligand O3 ( $\Delta E = +1.7 \text{ kJ mol}^{-1}$ , Fe–N–O<sub>calcd</sub> = 157°) is slightly less stable, as is a nitrosyl tilt towards the amine N atom N3 ( $\Delta E = +0.9 \text{ kJ mol}^{-1}$ , Fe–N–O<sub>calcd</sub> = 164°). In the least stable conformation, the NO ligand was tilted towards the aqua ligand, which, however, results in the lineation of the FeNO group ( $\Delta E = +2.0 \text{ kJ mol}^{-1}$ ). For **3**, similar results were obtained, the least stable position stemming from the tilt of the nitrosyl group towards the hydroxyethyl function.

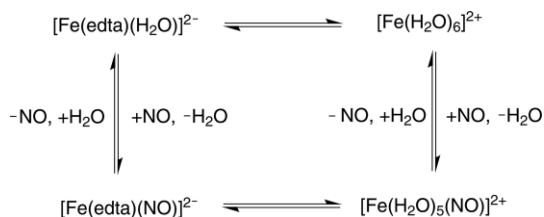
### Stability of the Fe–NO Linkage in Aqueous Solution

So far, some structural characteristics of a stable Fe–NO linkage have become obvious. Notably, the steric demand of a nitrosyl ligand is considerable. Thus, the reaction of the  $[\text{Fe}(\text{edta}-\kappa^2\text{N},\kappa^4\text{O})(\text{H}_2\text{O})]^{2-}$  educt to the  $[\text{Fe}(\text{edta}-\kappa^2\text{N},\kappa^3\text{O})(\text{NO})]^{2-}$  product species goes along with a decrease of the coordination number from seven to six, despite the fact that one of the chelating ligand's functional groups dangles. Obviously, an aqua ligand is sterically less demanding than a nitrosyl ligand. Accordingly, the molecular structures depicted in this work show the nitrosyl ligand in an environment of co-ligating atoms that are bent away from the NO group, thus supporting the observed short Fe–NO  $\sigma/\pi$  interaction (cf. the typical 1.78 Å Fe–N distance with the 2.27 Å Fe–O<sub>aq</sub> distance in the heptacoordinate educt complex<sup>[7c]</sup>). In agreement with these rules, six-membered chelate rings, which push the equatorial atoms towards the NO hemisphere, result in unstable FeNO moieties.<sup>[4]</sup> However, both the more stable Fe–NO links of the compounds of this work and the less stable representatives of our accompanying work belong to the same class of five-membered-ring chelates. Moreover, structural parameters such as Fe–N<sub>NO</sub> distances are similar. Hence, what is the reason for the different stabilities in aqueous solution?

Two points have to be considered, the first dealing with aqueous equilibria. With co-ligands of small denticity, the higher residual concentration of the less stable  $[\text{Fe}(\text{H}_2\text{O})_5(\text{NO})]^{2+}$  species in solutions of less stable co-ligand-iron(II) complexes seems responsible for the loss of NO from solutions exposed to an inert-gas stream, merely by the decomposition of the aquated species followed by equilibrium readjustment.

Scheme 2 summarises the relevant equilibria for the edta co-ligand. The edta-containing species are rather stable ( $\lg \beta_{\text{ML}} = 14.94$  at 0.1 mol L<sup>-1</sup> ionic strength),<sup>[10]</sup> hence the dominant left-hand side of Scheme 2 allows for only minor quantities of both aqua species. Replacing the multidentate edta ligand by the tridentate ida (iminodiacetate), as an example of a ligand that is not able to support stable solutions, changes the picture. The stability constant of the 1:1 species ( $\lg \beta_{\text{ML}} = 5.45$  at 1 mol L<sup>-1</sup> ionic strength)<sup>[11]</sup> indicates that the aminodicarboxylate complex is about ten orders of magnitude less stable. In solutions of this ligand, a less stable aminocarboxylate complex causes higher amounts of residual aqua complex. After NO absorption, the situation seems to be qualitatively the same, that is, the

green nitrosyl–iron solutions contain more (instable) or less (stable) aqua complex which is destroyed on stripping. On continuous readjustment of the solution equilibria, a less stable aminocarboxylate complex forms a less stable Fe/NO species due to a higher amount of the markedly instable aqua ion  $[\text{Fe}(\text{H}_2\text{O})_5(\text{NO})]^{2+}$ .



Scheme 2. Equilibria in aqueous  $\text{Fe}^{\text{II}}/\text{edta}/\text{NO}$  solutions.

The second aspect deals with structural parameters. It has been stated that, at first glance, the structures hardly mirror the stabilities. However, a closer look at structural parameters supports the suggestion that the Fe–NO stability is correlated to the higher weight of the trivalent state of the central metal atom. It was shown in ref.<sup>[11]</sup> that, supporting the computational results, the mean metal–co-ligand distances, with and without bonded nitric oxide, mirror the valence states of the central atoms.

The bhedda ligand provides a further example for this reasoning.  $[\text{Fe}(\text{bhedda}-\kappa^2\text{N},\kappa^4\text{O})]$  crystallised from NO-free batches. In the crystal structure, the NO-binding site is occupied by the carboxylate function from an adjacent coordination entity. The mean Fe–O<sub>carboxylate</sub> distance is 2.105 Å for the NO-free educt; the same parameter for nitrosyl compound **3** is markedly shorter, namely 2.050 Å. To quantify the weight of the ferric character, ferrous and ferric entities of the same overall structure may be considered. Among the aminocarboxylates, structural data for both ferrous and ferric complexes are available for heptacoordinate edta species. In  $[\text{Fe}^{\text{III}}(\text{edta})(\text{H}_2\text{O})]^-$ , the mean Fe–O distance is 2.121 Å;<sup>[12]</sup> in  $[\text{Fe}^{\text{II}}(\text{edta})(\text{H}_2\text{O})]^{2-}$ , the mean distance is 2.237 Å.<sup>[7c]</sup> The difference between the mean distances is 0.115 Å, which is, as expected, due to some degree of covalency in the Fe–O bonds – a bit smaller than the difference of the high-spin ionic radii for hexacoordinate ferrous and ferric centres of 0.145 Å.<sup>[13]</sup> As a result, the ferric  $\text{Fe}^{\text{III}}(\text{NO}^-)$  mesomer contributes a weight of roughly one half to the electronic state of **3**. The result seems to be typical for the class of aminocarboxylate-supported and, generally, anion-supported quartet- $\{\text{FeNO}\}^7$  centres.

The same consideration produces a different result for the aqua species. The data for the reference hexaaquaferrous and ferric complexes are: Fe<sup>III</sup>–O<sub>aq</sub> 1.995 Å (in caesium iron alum);<sup>[14]</sup> Fe<sup>II</sup>–O<sub>aq</sub> 2.124 Å (in ferrous sulfate heptahydrate).<sup>[15]</sup> The difference between the mean distances is 0.129 Å. Calculated values [BP86/def2-TZVP, dispersion correction, COSMO(water)] are close to the experimental data: 2.015 Å for the hexaaquaferrous ion, 2.122 Å for the ferrous analogue, with a difference of 0.115 Å. The thus reliably calculated values can then be completed by the mean Fe–O distance in the experimentally (still) inaccessible  $[\text{Fe}(\text{H}_2\text{O})_5(\text{NO})]^{2+}$  ion: 2.125 Å, indicating a pure ferrous state for this least stable nitrosyl derivative. On the one

hand, in the less stable class, the same result, namely a pure ferrous state, was found for the dipic co-ligand. On the other hand, ferric admixture was demonstrated for the oxodiacetato (oda) co-ligand despite the fact that the nitrosyl moiety was of limited stability. This latter result shows that the two criteria for a stable FeNO complex – well-suited aqueous equilibria in the sense of Scheme 2 and a considerable weight of the ferric state – have to be met at the same time.

A final look should be taken at the left-hand side of the equilibria in Scheme 2. The edta ligand is potentially hexadentate. As the crystal structure shows, NO binding requires one edta function to dangle. NO is thus the competitor to a reliably ligating function, which, moreover, is part of a chelate. Obviously, a hemilabile function would perform better in terms of stable NO coordination. In fact, the hedtra ligand, which was derived from edta by replacing one carboxymethyl by a hydroxyethyl function, supported NO binding best in van Eldik's survey.<sup>[4c]</sup>

## Conclusions

We have presented crystal-structure analyses of four  $\{\text{FeNO}\}^7(S = 3/2)$  complexes with polydentate aminocarboxylate co-ligands. The aqueous solutions of these species share the peculiarity that they are stable against NO loss upon stripping with inert gas or upon the application of vacuum. Related aminocarboxylate analogues of lower denticity lead to instability towards NO loss, despite the fact that experimental and computed structural data of stable and instable aminocarboxylate derivatives are essentially the same in terms of distances and angles for the investigated quartet- $\{\text{FeNO}\}^7$  centres.

As a consequence, instability towards NO loss on stripping is observed as a result of a higher amount of the instable  $[\text{Fe}(\text{H}_2\text{O})_5(\text{NO})]^{2+}$  ion in the aqueous solution equilibria. In terms of structural parameters, this dication resembles a pure ferrous state (as does a dipic derivative), whereas the aminocarboxylate-supported centres show considerable admixture of the ferric  $\text{Fe}^{\text{III}}(\text{NO}^-)$  mesomer, which, however, is not a sufficient condition for FeNO stability in aqueous solution. Keeping in mind the goal of ligand optimisation towards preferential NO binding, the knowledge of the structures adds new criteria. With the finding that the coordination number of a multidentate co-ligand such as edta changes from seven to six on NO binding, new ligands such as potentially heptadentate, bis(hemilabile) chelators may be tailored.

## Experimental Section

### General Remarks and Synthetic Route to the Crystalline $\{\text{FeNO}\}^7(S = 3/2)$ Complexes

Due to the possible oxidation of  $\text{FeSO}_4 \cdot 7\text{H}_2\text{O}$  and the synthesised  $\{\text{FeNO}\}^7(S = 3/2)$  compounds, all experiments were carried out under strict exclusion of oxygen from air by using standard Schlenk techniques with argon as the inert gas. Solvents were deaerated with argon before usage.  $\text{FeSO}_4 \cdot 7\text{H}_2\text{O}$ ,  $\text{H}_2\text{edda}$ ,  $\text{H}_3\text{nnta}$ ,  $\text{H}_4\text{edta}$ , sodium hydroxide and potassium hydroxide were purchased from Sigma Aldrich, Acros, Fluka or Grüssing.  $\text{H}_2\text{bhedda}$  was synthesised

according to a slightly modified published procedure by Wensel and Meares.<sup>[16]</sup> Nitric oxide was supplied by Air Liquide.

To enable the crystallisation of the  $\{\text{FeNO}\}^7(S = 3/2)$  complexes, the principle of isothermal diffusion was utilised. In this context, a two-chamber Schlenk flask was constructed by integrating a test tube into a conventional Schlenk tube. The reaction partners were dissolved inside the test tube while a suitable solvent with less polarity was added outside to diffuse into the reaction solution.

Nitric oxide was purged with a sodium hydroxide solution (4 M) before passing it through the reaction flask to exclude higher oxidised NO species and polymers. Excess NO gas was converted to  $\text{N}_2$  with an amidosulfuric acid solution (2 M). Because of the strong absorption band of water in the region of the characteristic NO stretching vibration, IR spectra of the dissolved complexes were recorded in  $\text{D}_2\text{O}$ .

**$[\text{Fe}(\text{edda})(\text{H}_2\text{O})(\text{NO})]\cdot 0.5\text{H}_2\text{O} = 1\cdot 0.5\text{H}_2\text{O}$ :** Sodium hydroxide (0.100 g, 2.50 mmol) was added to a suspension of  $\text{H}_2\text{edda}$  (0.220 g, 1.25 mmol) in distilled water (4 mL). The mixture was stirred for 30 min at room temperature.  $\text{FeSO}_4\cdot 7\text{H}_2\text{O}$  (0.278 g, 1.00 mmol) was added in portions, and a slightly green solution resulted. The solution was treated with gaseous nitric oxide for ten minutes, whereby a colour change to green-black was observed after two minutes. The green-black solution was stored at room temperature under an NO atmosphere, and over three weeks, acetone (4 mL) was diffused into the reaction solution.  $[\text{Fe}(\text{edda})(\text{H}_2\text{O})(\text{NO})]\cdot 0.5\text{H}_2\text{O}$  (0.121 g, 42 %) was isolated in the form of black crystals. IR (crystal, ATR):  $\tilde{\nu} = 2360$  (vs), 2341 (vs), 1761 (m,  $\nu_{\text{NO}}$ ), 1589 (s), 1457 (w), 1417 (w), 1376 (m), 1339 (m), 1306 (w), 1282 (vw), 1248 (vw), 1213 (vw), 1141 (w), 1117 (vw), 1075 (vw), 1016 (w), 958 (m), 913 (w)  $\text{cm}^{-1}$ . IR (reaction solution,  $\text{D}_2\text{O}$ , measuring cell with  $\text{CaF}_2$  panels):  $\tilde{\nu} = 1769$  (s,  $\nu_{\text{NO}}$ ), 1599 (vs), 1462 (vs), 1389 (vs), 1320 (s), 1291 (w)  $\text{cm}^{-1}$ . UV/Vis (crystal):  $\lambda = 414, 430, 644$  nm. UV/Vis (reaction solution, 1 mmol  $\text{L}^{-1}$ ):  $\lambda = 342, 435$  nm. UV/Vis (reaction solution, 10 mmol  $\text{L}^{-1}$ ):  $\lambda = 617$  nm.

**$[\{\text{Fe}(\text{H}_2\text{O})_4\}\{\text{Fe}(\text{NO})(\text{nta})\}_2]_{n/n}\cdot 2\text{H}_2\text{O} = [\text{Fe}(\text{H}_2\text{O})_4(2)]_{n/n}\cdot 2\text{H}_2\text{O}$ :** To a suspension of  $\text{H}_3\text{nta}$  (0.194 g, 1.00 mmol) in distilled water (3 mL) was added sodium hydroxide (0.086 g, 2.15 mmol). After stirring the colourless solution for 30 min at room temperature,  $\text{FeSO}_4\cdot 7\text{H}_2\text{O}$  (0.278 g, 1.00 mmol) was added to it in portions. Nitric oxide was bubbled through the slightly green solution for ten minutes, and a green-black solution resulted. The mixture was stored at room temperature under an NO atmosphere, and over six months, acetone (6 mL) was diffused into the reaction solution. The NO atmosphere was changed to an argon atmosphere, and ethanol (6 mL) was added to diffuse over a further six months into the reaction solution. After a period of one year,  $[\{\text{Fe}(\text{H}_2\text{O})_4\}\{\text{Fe}(\text{NO})(\text{nta})\}_2]_{n/n}\cdot 2\text{H}_2\text{O}$  (0.173 g, 48 %) was isolated in the form of large black crystals suitable for X-ray crystallography. IR (crystal, ATR):  $\tilde{\nu} = 3222$  (s), 1791 (s,  $\nu_{\text{NO}}$ ), 1574 (vs), 1505 (vs), 1459 (m), 1317 (s), 1271 (s), 1223 (m), 1124 (m), 912 (w), 736 (s)  $\text{cm}^{-1}$ . IR (reaction solution,  $\text{D}_2\text{O}$ , measuring cell with  $\text{CaF}_2$  panels):  $\tilde{\nu} = 1793$  (w,  $\nu_{\text{NO}}$ ), 1714 (s), 1623 (vs), 1435 (s), 1400 (vs), 1319 (m), 1280 (m), 1255 (m), 1240 (w)  $\text{cm}^{-1}$ . UV/Vis (crystal):  $\lambda = 433, 622$  nm. UV/Vis (reaction solution, 3 mmol  $\text{L}^{-1}$ ):  $\lambda = 339, 439, 602$  nm.

### **$[\text{Fe}(\text{bhedda})(\text{NO})]$ (3)**

$\text{H}_2\text{bhedda}$  was synthesised by following a published procedure by Wensel and Meares<sup>[16]</sup> under an  $\text{N}_2$  atmosphere. *N,N'*-bis(2-hydroxyethyl)-*N,N'*-ethylenediamine (2.51 g, 18.0 mmol) was dissolved in distilled water (8 mL). The solution was cooled with an ice bath, and bromoacetic acid (5.02 g, 36.0 mmol) was added in portions while stirring. During the addition of bromoacetic acid, the pH value

of the mixture was kept at 11 with aqueous potassium hydroxide solution (7 M). The resulting mixture was stirred at 40 °C for 60 h, whereby the pH value was still maintained at 10–11. The colourless reaction solution was treated with  $\text{FeSO}_4\cdot 7\text{H}_2\text{O}$  (5.00 g, 18.0 mmol) to form the  $[\text{Fe}^{\text{II}}(\text{bhedda})]$  complex. The white solid that precipitated was filtered from the reaction solution and dried in vacuum to give 1.26 g (22 %) of a white solid containing the  $[\text{Fe}^{\text{II}}(\text{bhedda})]$  complex. For the subsequent reaction with nitric oxide, the solid was utilised without further purification. By diffusion of acetone over two weeks,  $[\text{Fe}^{\text{II}}(\text{bhedda})]$  was crystallised from an aqueous solution as colourless needle-shaped crystals suitable for X-ray crystallography (see the Supporting Information for details). MS  $\{\text{FAB}, M = [\text{Fe}^{\text{II}}(\text{bhedda})]\}$ :  $\text{FAB}^+ m/z = 319.2 [M + \text{H}]^+$ ,  $\text{FAB}^- m/z = 317.2 [M - \text{H}]^-$ .

The white  $[\text{Fe}^{\text{II}}(\text{bhedda})]$  complex (0.300 g, 0.940 mmol) was dissolved in water (3 mL). Gaseous nitric oxide was bubbled through the light-green solution for ten minutes, and, after two minutes, a colour change to green-black was observed, indicating the formation of the  $\{\text{FeNO}\}^7$  chromophore. All attempts to crystallise  $[\text{Fe}(\text{bhedda})(\text{NO})]$  from an aqueous solution failed. Instead, the crystallisation of the complex succeeded from a methanol solution.  $[\text{Fe}^{\text{II}}(\text{bhedda})]$  (0.050 g, 0.157 mmol) was dissolved in methanol (1 mL), and the solution was treated with gaseous nitric oxide. The resulting brown-black reaction solution was stored at room temperature under an NO atmosphere, and acetone (2 mL) was diffused over two weeks into the reaction solution.  $[\text{Fe}(\text{bhedda})(\text{NO})]$  was isolated as one single black crystal. IR (crystal): reaction yield too low. IR (reaction solution,  $\text{D}_2\text{O}$ , measuring cell with  $\text{CaF}_2$  panels):  $\tilde{\nu} = 1782$  (m,  $\nu_{\text{NO}}$ ), 1620 (s), 1380 (w)  $\text{cm}^{-1}$ . UV/Vis (crystal): reaction yield too low. UV/Vis (reaction solution,  $\text{H}_2\text{O}$ , 3 mmol  $\text{L}^{-1}$ ):  $\lambda = 337, 422, 650$  nm.

**$[\text{Fe}(\text{H}_2\text{O})_2(\text{Fe}(\text{NO})(\text{Hedta}))_2]_{n/n} = [\text{Fe}(\text{H}_2\text{O})_2(4)]_{n/n}$ :** To  $\text{H}_4\text{edta}$  (0.292 g, 1.00 mmol) in distilled water (3 mL) was added 85 % potassium hydroxide (0.187 g, 3.33 mmol), and the colourless solution was stirred for 30 min at room temperature.  $\text{FeSO}_4\cdot 7\text{H}_2\text{O}$  (0.278 g, 1.00 mmol) was added in portions, and a slightly green solution resulted. Gaseous nitric oxide was bubbled through the reaction solution for ten minutes, whereby, after two minutes, the characteristic colour change to green-black was observed. The solution was stored at room temperature under an NO atmosphere, and acetone (3 mL) was diffused into the reaction solution over six months.  $[\text{Fe}(\text{H}_2\text{O})_2(\text{Fe}(\text{NO})(\text{Hedta}))_2]_{n/n}$  (0.347 g, 82 %) was isolated in the form of large black crystals. IR (crystal, ATR):  $\tilde{\nu} = 3255$  (vw), 2968 (vw), 1839 (w), 1781 (m,  $\nu_{\text{NO}}$ ), 1572 (s), 1440 (w), 1370 (s), 1316 (m), 1260 (vw), 1215 (w), 1168 (m), 1102 (s), 1024 (vw), 1002 (w), 979 (w), 931 (m), 861 (w), 800 (w), 717 (m), 685 (m)  $\text{cm}^{-1}$ . IR (reaction solution,  $\text{D}_2\text{O}$ , measuring cell with  $\text{CaF}_2$  panels):  $\tilde{\nu} = 1777$  (s,  $\nu_{\text{NO}}$ ), 1643 (vs), 1592 (vs), 1466 (s), 1439 (s), 1403 (vs), 1384 (vs), 1321 (s), 1269 (w), 1289 (s), 1234 (s), 1218 (s), 1205 (s)  $\text{cm}^{-1}$ . UV/Vis (crystal):  $\lambda = 432, 623$  nm. UV/Vis (reaction solution, 3 mmol  $\text{L}^{-1}$ ):  $\lambda = 342, 435, 634$  nm.

**Computational Chemistry:** DFT calculations were run with TURBOMOLE<sup>[17]</sup> {ORCA<sup>[18]</sup> in the case of the tentative ferrate  $[\text{FeF}_3(\text{NH}_3)_2(\text{NO})]^-$  with starting geometries obtained from X-ray diffraction using the basis set def2-TZVP<sup>[19]</sup> and the functionals TPSSH<sup>[20]</sup> or BP86.<sup>[21]</sup> All calculations were performed using spin-unrestricted open-shell systems with a quartet spin state. COSMO<sup>[22]</sup> was applied for solvent correction and the dispersion correction by Grimme<sup>[23]</sup> was used. In case of the Fe–N–O bending potential of  $[\text{Fe}(\text{bhedda})(\text{NO})]$  (cf. Figure 5), the Fe–N–O angles were fixed to constrained values while optimising all other coordinates, that is, a relaxed scan was performed.

## X-ray Diffraction

Crystals were selected by using a Leica MZ6 polarisation microscope. Suitable crystals were measured with single-crystal diffractometers of the types Bruker Nonius Kappa CCD, Bruker D8 Quest and Bruker D8 Venture using Mo- $K_{\alpha}$  irradiation. The structure solutions were carried out by direct methods using SHELXS; the structures were refined by full-matrix least-squares calculations on  $F^2$  using SHELXL and ShelXL.<sup>[24]</sup> Distances and angles were calculated with Platon.<sup>[25]</sup> For visualisation ORTEP was used.<sup>[26]</sup>

CCDC 1510621 (for **1**), 1510622 (for **2**), 1510624 (for **3**), and 1510623 (for **4**) contain the supplementary crystallographic data for this paper. These data can be obtained free of charge from The Cambridge Crystallographic Data Centre.

## Acknowledgments

The authors gratefully acknowledge financial support from the Deutsche Forschungsgemeinschaft (DFG) priority program SPP1740, which deals with the “influence of local transport processes in chemical reactions in bubble flows”.

**Keywords:** Iron · Nitrosyl ligands · Chelates · Density functional calculations · Structure elucidation

- [1] M. Wolf, P. Klüfers, *Eur. J. Inorg. Chem.* **2017**, 2303–2312.
- [2] D. Littlejohn, S. G. Chang, *Ind. Eng. Chem. Res.* **1987**, *26*, 1232–1234.
- [3] a) Y. Zhang, M. A. Pavlosky, C. A. Brown, T. E. Westre, B. Hedman, K. O. Hodgson, E. I. Solomon, *J. Am. Chem. Soc.* **1992**, *114*, 9189–9191; b) T. E. Westre, A. Di Cicco, A. Filippini, C. R. Natoli, B. Hedman, E. I. Solomon, K. O. Hodgson, *J. Am. Chem. Soc.* **1994**, *116*, 6757–6768; c) C. A. Brown, M. A. Pavlosky, T. E. Westre, Y. Zhang, B. Hedman, K. O. Hodgson, E. I. Solomon, *J. Am. Chem. Soc.* **1995**, *117*, 715–732.
- [4] a) T. Schnepf, S. Finkler, A. Czap, R. van Eldik, M. Heus, P. Nieuwenhuizen, C. Wreesmann, W. Abma, *Eur. J. Inorg. Chem.* **2001**, 491–501; b) T. Schnepf, A. Wanat, G. Stochel, S. Goldstein, D. Meyerstein, R. van Eldik, *Eur. J. Inorg. Chem.* **2001**, 2317–2325; c) T. Schnepf, A. Wanat, G. Stochel, R. van Eldik, *Inorg. Chem.* **2002**, *41*, 2565–2573; d) M. Wolak, R. van Eldik, *Coord. Chem. Rev.* **2002**, *230*, 263–282.
- [5] a) Y. Xia, J. Zhao, M. Li, S. Zhang, S. Li, W. Li, *Environ. Sci. Technol.* **2016**, *50*, 3846–3851; b) W. Li, J. Zhao, L. Zhang, Y. Xia, N. Liu, S. Li, S. Zhang, *Scientific Reports* **2016**, *6*, Article number: 18876; c) J. Chen, L. Wang, J. Zheng, J. Chen, *Bioprocess Biosyst. Eng.* **2015**, *38*, 1373–1380; d) N. Liu, Y. Jiang, L. Zhang, Y. Xia, B. Lu, B. Xu, W. Li, S. Li, *Energy Fuels* **2014**, *28*, 7591–7598; e) Y. Xia, Y. Shi, Y. Zhou, N. Liu, W. Li, S. Li, *Energy Fuels* **2014**, *28*, 3332–3338; f) C. de Salas, M. R. Heinrich, *Green Chem.* **2014**, *16*, 2982–2987; g) H. Niu, D. Y. C. Leung, *Environ. Rev.* **2010**, *18*, 175–189; h) P. van der Maas, L. Harmsen, S. Weelink, B. Klapwijk, P. Lens, *J. Chem. Technol. Biotechnol.* **2004**, *79*, 835–841; i) P. van der Maas, T. van de Sandt, B. Klapwijk, P. Lens, *Biotechnol. Prog.* **2003**, *19*, 1323–1328.
- [6] J. Maigut, R. Meier, R. van Eldik, *Inorg. Chem.* **2008**, *47*, 6314–6321.
- [7] a) T. Mizuta, J. Wang, K. Miyoshi, *Bull. Chem. Soc. Jpn.* **1993**, *66*, 2547–2551; b) T. Mizuta, J. Wang, K. Miyoshi, *Inorg. Chim. Acta* **1995**, *230*, 119–125; c) H.-M. Huang, H.-B. Yang, X.-Y. Li, F.-F. Ren, *Acta Crystallogr., Sect. E* **2009**, *65*, m87–m88.
- [8] a) K. Pohl, K. Wieghardt, B. Nuber, J. Weiss, *J. Chem. Soc., Dalton Trans.* **1987**, 187–192; b) C. R. Randall, Y. Zang, A. E. True, L. Que Jr., J. M. Charnock, C. D. Garner, Y. Fujishima, C. J. Schofield, J. E. Baldwin, *Biochemistry* **1993**, *32*, 6664–6673; c) Y.-M. Chiou, L. Que Jr., *Inorg. Chem.* **1995**, *34*, 3270–3278; d) A. L. Feig, M. T. Bautista, S. J. Lippard, *Inorg. Chem.* **1996**, *35*, 6892–6898; e) C. Hauser, T. Glaser, E. Bill, T. Weyhermüller, K. Wieghardt, *J. Am. Chem. Soc.* **2000**, *122*, 4352–4365; f) M. Li, D. Bonnet, E. Bill, F. Neese, T. Weyhermüller, N. Blum, D. Sellmann, K. Wieghardt, *Inorg. Chem.* **2002**, *41*, 3444–3456; g) B. Weber, H. Görls, M. Rudolph, E. G. Jäger, *Inorg. Chim. Acta* **2002**, *337*, 247–265; h) D. P. Klein, V. G. Young Jr., W. B. Tolman, L. Que Jr., *Inorg. Chem.* **2006**, *45*, 8006–8008; i) F. Te Tsai, P. L. Chen, W. F. Liaw, *J. Am. Chem. Soc.* **2010**, *132*, 5290–5299; j) T. C. Berto, M. B. Hoffman, Y. Murata, K. B. Landenberger, E. E. Alp, J. Zhao, N. Lehnert, *J. Am. Chem. Soc.* **2011**, *133*, 16714–16717; k) G. Villar-Acevedo, E. Nam, S. Fitch, J. Benedict, J. Freudenthal, W. Kaminsky, J. A. Kvas, *J. Am. Chem. Soc.* **2011**, *133*, 1419–1427; l) H. Park, M. M. Bittner, J. S. Baus, S. V. Lindeman, A. T. Fiedler, *Inorg. Chem.* **2012**, *51*, 10279–10289; m) A. Majumdar, S. J. Lippard, *Inorg. Chem.* **2013**, *52*, 13292–13294; n) F. Te Tsai, Y. C. Lee, M. H. Chiang, W. F. Liaw, *Inorg. Chem.* **2013**, *52*, 464–473; o) S. Zheng, T. C. Berto, E. W. Dahl, M. B. Hoffman, A. L. Speelman, N. Lehnert, *J. Am. Chem. Soc.* **2013**, *135*, 4902–4905; p) J. Li, A. Banerjee, P. L. Pawlak, W. W. Brennessel, F. A. Chavez, *Inorg. Chem.* **2014**, *53*, 5414–5416; q) E. Victor, S. Kim, S. J. Lippard, *Inorg. Chem.* **2014**, *53*, 12809–12821; r) E. Victor, M. A. Minier, S. J. Lippard, *Eur. J. Inorg. Chem.* **2014**, 5640–5645.
- [9] P. Kubelka, *J. Opt. Soc. Am.* **1948**, *38*, 1067.
- [10] N. Clark, A. Martell, *Inorg. Chem.* **1988**, *27*, 1297–1298.
- [11] K. Micskei, *J. Chem. Soc., Dalton Trans.* **1987**, 255–257.
- [12] R. Meier, F. W. Heinemann, *Inorg. Chim. Acta* **2002**, *337*, 317–327.
- [13] R. Shannon, *Acta Crystallogr., Sect. A* **1976**, *32*, 751–767.
- [14] J. K. Beattie, S. P. Best, B. W. Skelton, A. H. White, *J. Chem. Soc., Dalton Trans.* **1981**, 2105–2111.
- [15] F. R. Fronczek, S. N. Collins, J.-Y. Chan, *Acta Crystallogr., Sect. E* **2001**, *57*, i26–i27.
- [16] T. G. Wensel, C. F. Meares, *Biochemistry* **1983**, *22*, 6247–6254.
- [17] TURBOMOLE V6.6 **2014**, a development of University of Karlsruhe and Forschungszentrum Karlsruhe GmbH, 1989–2007, TURBOMOLE GmbH, since 2007; available from <http://www.turbomole.com>; R. Ahlrichs, M. Bär, M. Häser, H. Horn, C. Kölmel, *Chem. Phys. Lett.* **1989**, *162*, 165–169.
- [18] F. Neese, *ORCA* – an ab initio, density functional and semiempirical program package, Version 2.9 University of Bonn, **2006**.
- [19] F. Weigend, R. Ahlrichs, *Phys. Chem. Chem. Phys.* **2005**, *7*, 3297–3305.
- [20] J. Tao, J. P. Perdew, V. N. Staroverov, G. E. Scuseria, *Phys. Rev. Lett.* **2003**, *91*, 146401.
- [21] a) A. D. Becke, *Phys. Rev. A* **1988**, *38*, 3098–3100; b) J. P. Perdew, *Phys. Rev. B* **1986**, *33*, 8822–8824.
- [22] A. Klamt, G. Schüürmann, *J. Chem. Soc., Perkin Trans. 2* **1993**, *5*, 799–805.
- [23] S. Grimme, *J. Comput. Chem.* **2006**, *27*, 1787–1799.
- [24] a) G. Sheldrick, *Acta Crystallogr., Sect. A* **2008**, *64*, 112–122; b) C. B. Hübschle, G. M. Sheldrick, B. Dittrich, *J. Appl. Crystallogr.* **2011**, *44*, 1281–1284.
- [25] A. Spek, *J. Appl. Crystallogr.* **2003**, *36*, 7–13.
- [26] L. Farrugia, *J. Appl. Crystallogr.* **1997**, *30*, 565.

Received: November 4, 2016